

***Dynamics of a hybrid thermostat model with  
discrete sampling time control***

Glendinning, Paul and Kowalczyk, Piotr

2008

MIMS EPrint: **2008.102**

Manchester Institute for Mathematical Sciences  
School of Mathematics

The University of Manchester

Reports available from: <http://eprints.maths.manchester.ac.uk/>

And by contacting:  
The MIMS Secretary  
School of Mathematics  
The University of Manchester  
Manchester, M13 9PL, UK

ISSN 1749-9097

## RESEARCH ARTICLE

**Dynamics of a hybrid thermostat model with discrete sampling time control**Paul Glendinning <sup>a</sup> and Piotr Kowalczyk <sup>b\*</sup><sup>a</sup>Centre for Interdisciplinary Computational and Dynamical Analysis (CICADA) and School of Mathematics, University of Manchester, Oxford Road, Manchester M13 9PL, U.K.; <sup>b</sup>Centre for Interdisciplinary Computational and Dynamical Analysis (CICADA), School of Mathematics, University of Manchester, Oxford Road, Manchester M13 9PL,

U.K.

(Received 00 Month 200x; in final form 00 Month 200x)

The dynamics of a simple thermostat model is described. In the model the control system samples the temperature at regular but discrete time intervals rather than by continuous monitoring. The model exhibits quasi-periodic oscillations and banding, where the response falls into two or more bands of phase space representing either better or poorer control. A return circle map is derived which explains the observed dynamics. Some extensions of these results to the case where the flow is nonlinear are also given.

**Keywords:** hybrid systems; bifurcations; discrete sampling; circle maps

**AMS Subject Classification:** 37Dxx; 37Fxx; 37Gxx

**1. Background**

In recent years much research effort has been directed toward understanding the dynamics of systems characterized by continuous and discrete evolution, e.g. [1–4]. Such systems are often called hybrid dynamical systems [5] and examples of relevance to engineering applications include models of DC/DC power converters [6], control systems with an on/off control where the switch is assumed to occur instantaneously [7], systems with impacts [8–11], and friction [12, 13]. It has been shown that the interaction between the continuous and discrete dynamics often leads to abrupt transitions [14] which are triggered by the hybrid character of the system.

In this paper we consider a simple on/off hybrid control system with a modified, digital, rule that determines the switching. When on/off control systems are treated in the control literature it is usually assumed that information of the value of some control variable,  $y(t)$  say, is available at the same time instant  $t$  [15]. Therefore an ideal switch changes the system between an on and off state, and *vice versa*, at precisely the time when some threshold value is reached. In some applications measurement may be expensive, or is performed digitally, and then it may be reasonable to suppose that the value of the control variable  $y(t)$  is only available at some discrete set of sampling times. In such cases the system will not switch between different configurations when the threshold value of the control variable

---

\*Corresponding author. Email: piotr.kowalczyk@manchester.ac.uk

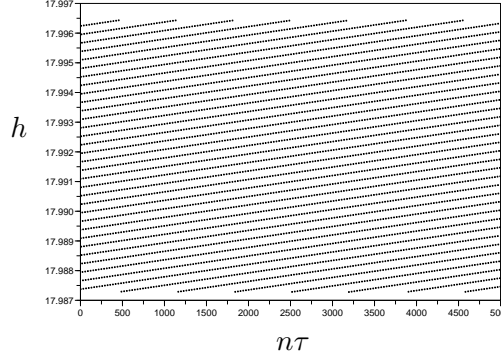


Figure 1. Values of  $h$  of the return map (10) at times  $n\tau$  for  $n = 1, 2, 3, \dots, 5000$  with  $h_1 = 18$ ,  $h_2 = 22$ ,  $r_1 = 0.2$ ,  $r_2 = 2\sqrt{2}/100$  and  $\tau = (1 + \sqrt{5})/10$ . Iterates appear to lie within a single band of allowed values.

is reached but at the first sample time at which the control variable that is greater than the set threshold. The aim of this paper is to describe how such a modification of the control strategy alters the system dynamics.

The paper is organized as follows. In Section 2 a simple one-dimensional on/off model of a control system with an instantaneous switching law and continuous time monitoring of the control variable  $y(t)$  is described and a modification to the model which introduces discrete time sampling of the control variable is introduced. Numerical simulations are used to show some of the effects of such a modification. In Section 3 a return map is derived and two generic cases of maps that can be reduced to circle maps are analyzed. In Section 4 we present a methodology that allows for an exhaustive treatment of all the possible scenarios, although only the more tractable cases are chosen for the analysis. The ones which are left unexplored can be analyzed using the same principles, but the proliferation of cases makes a complete description unwieldy. In Section 6 we present a generalization of some of the results to the case when instead of a linear evolution a generic nonlinear function is assumed to govern the system dynamics in between switching events. Finally, in Section 7 we conclude the paper, and further directions of research instigated by the presence of discrete sampling which we consider to be an important and as yet unexplored feature of hybrid systems, are indicated.

## 2. The model thermostat

Simple models of thermostat control are frequently used as illustrations of hybrid systems. The most elementary of these fixes two thresholds and turns on a heater if the temperature falls below the lower threshold and turns off the heater if the temperature rises above the higher threshold. The control system is described as hybrid because it couples a continuous state variable for the temperature with a discrete variable (on/off) for the state of the control system. The standard model of a thermostat control has the temperature,  $h$ , varying as  $\dot{h} = -ah$  is off, and  $\dot{h} = -a(h - d)$  if the control is on for appropriate choices of  $a, d > 0$ . Here we consider a simplification with

$$\frac{dh}{dt} = \begin{cases} r_1 & \text{if } c = \text{on} \\ -r_2 & \text{if } c = \text{off} \end{cases} \quad (1)$$

where  $r_i$ ,  $i = 1, 2$  are positive constants representing the rate of heating or cooling of the room. The state of  $c$  changes from on to off if  $h$  rises above a threshold  $h_2$  and from off to on if  $h$  falls below  $h_1$ , with  $h_1 < h_2$ .

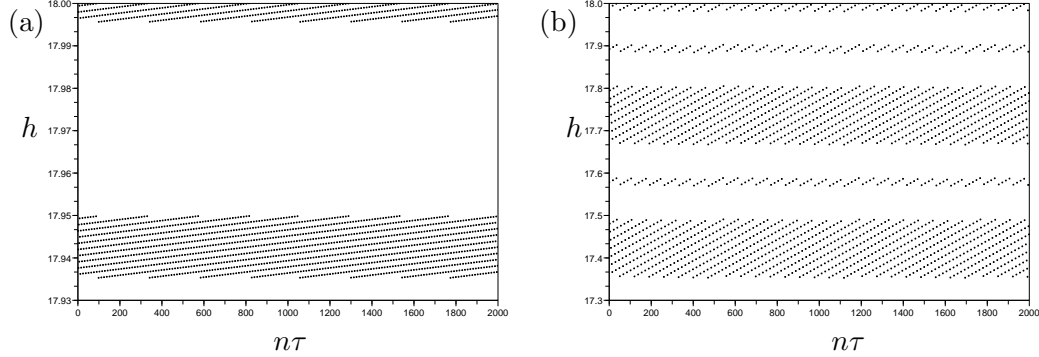


Figure 2. The values of  $h$  of the return map (10) at times  $n\tau$  for  $n = 1, 2, 3 \dots, 2000$  with parameters as in Figure 2 except (a)  $r_2 = \sqrt{2}/10$ ,  $\tau = (1 + \sqrt{5})/10$ , and (b)  $r_2 = 3\sqrt{2}/10$ ,  $\tau = 1 + \sqrt{5}$ . Note the banded structure, with ranges of values of  $h$  which are not visited by iterates of the map.

If the control acts instantaneously it is an elementary exercise to show that once it is in operation the system is periodic; choosing the origin of time to be at a moment when  $h = h_1$  then for  $t > 0$

$$h(t) = \begin{cases} h_1 + r_1(t - T_{2n}) & \text{if } t \in [T_{2n}, T_{2n+1}] \\ h_2 - r_2(t - T_{2n+1}) & \text{if } t \in [T_{2n+1}, T_{2(n+1)}] \end{cases} \quad (2)$$

where

$$T_{2n} = (nr_1 + nr_2)(h_2 - h_1), \quad T_{2n+1} = ((n+1)r_1 + nr_2)(h_2 - h_1). \quad (3)$$

The temperature therefore oscillates regularly between the two thresholds with period  $(r_1 + r_2)(h_2 - h_1)$ .

There are many ways to complicate this simple model in an attempt to make it more realistic. The relaxation and heating of the temperature in (1) can be more sophisticated; exponential growth or decay from an ambient temperature is often used. The heating element may continue to heat the room after the unit is switched off because its elements take time to cool down. Alternatively, or in addition, the switching on and off of the control can be considered in more detail. For example there might be a random element to the switching [16] or the control may involve a time lag leading to a delayed equation [17]. In this paper an alternative complication is considered. It will be assumed that the control monitors the ambient temperature at regular but discrete times,  $n\tau$ , and immediately switches the control if either of the threshold inequalities  $h < h_1$  or  $h > h_2$  are satisfied at that time. Although this is not of immediate relevance to thermostats, one can imagine situations where continuous monitoring of a variable cannot be done either for technical reasons, or for reasons of economy, and the thermostat model provides a simple and well understood example of the ways in which the control operation can be changed under these circumstances. Note that this is half way towards the quantized models of [18, 19] where measurements in both space and time are discretized. The effects of the quantization of space including the effects of time delay in nonlinear control systems have been studied in [20].

Thus the model introduced here has an additional parameter  $\tau > 0$  which describes the time between successive samples of the temperature. If the temperature evolves according to (1) the control variable in the new model described above switches from **on** to **off** at  $n\tau$  if  $c(n\tau) = \text{on}$  and  $h(n\tau) > h_2$ , in which case  $c(n\tau_+) = \text{off}$  (where  $c(s_+) = \lim_{t \downarrow s} c(t)$ ) and similarly it switches from **off** to **on** at  $n\tau$  if  $c = \text{off}$  and  $h(n\tau) < h_1$ , in which case  $c(n\tau_+) = \text{on}$ . We have used strict

inequalities for mathematical convenience, as will become clear in the next paragraph when the model is analyzed using a return map technique. Once operational the temperature is restricted to the interval  $[h_1 - r_2\tau, h_2 + r_1\tau]$  so we can choose the origin of time so that  $h(0) \in [h_1 - r_2\tau, h_1]$ ,  $c(0) = \text{off}$  and  $c(0_+) = \text{on}$ . The heater will remain on until  $t = N_1\tau$  where

$$h(N_1\tau) = h(0) + N_1r_1\tau > h_2, \quad h(0) + (N_1 - 1)r_1\tau \leq h_2. \quad (4)$$

It will then switch off and the room will cool until  $t = N_2\tau$  where

$$h((N_1 + N_2)\tau) = h(N_1\tau) - N_2r_2\tau < h_1, \quad h(N_1\tau) - (N_2 - 1)r_2\tau \geq h_1. \quad (5)$$

Rearranging the two inequalities of (4) gives

$$N_1 - 1 \leq \frac{h_2 - h(0)}{r_1\tau}, \quad N_1 > \frac{h_2 - h(0)}{r_1\tau} \quad (6)$$

or

$$N_1 = \lfloor \frac{h_2 - h(0)}{r_1\tau} \rfloor + 1 = \lfloor \frac{h_2 + r_1\tau - h(0)}{r_1\tau} \rfloor \quad (7)$$

where  $\lfloor x \rfloor$  is the floor function, the largest integer less than or equal to  $x$  (this is where there is some convenience in the choice of strict inequality referred to in the opening paragraph of this section). Similarly

$$N_2 = \lfloor \frac{h(N_1\tau) - h_1}{r_2\tau} \rfloor + 1 = \lfloor \frac{h(N_1\tau) + r_2\tau - h_1}{r_2\tau} \rfloor. \quad (8)$$

Putting these together with (4) and (5) gives the simplified equations

$$\begin{aligned} h(N_1\tau) &= h(0) + r_1\tau \lfloor \frac{h_2 + r_1\tau - h(0)}{r_1\tau} \rfloor \\ h((N_1 + N_2)\tau) &= h(N_1\tau) - r_2\tau \lfloor \frac{h(N_1\tau) + r_2\tau - h_1}{r_2\tau} \rfloor \end{aligned} \quad (9)$$

Since  $h((N_1 + N_2)\tau) \in [h_1 - r_2\tau, h_1]$  as was  $h(0)$  we can now iterate this process to obtain the sequence  $h_0 = h(0), h_1 = h(N_1\tau), \dots$  of values of the temperature at switching points:

$$\begin{aligned} h_{2n+1} &= h_{2n} + r_1\tau \lfloor \frac{h_2 + r_1\tau - h_{2n}}{r_1\tau} \rfloor \\ h_{2n+2} &= h_{2n+1} - r_2\tau \lfloor \frac{h_{2n+1} + r_2\tau - h_1}{r_2\tau} \rfloor \end{aligned} \quad (10)$$

with  $h_{2n} \in [h_1 - r_2\tau, h_1]$  and  $h_{2n+1} \in (h_2, h_2 + r_1\tau]$ . Composing these we get a single equation for even switching levels as a function of the previous even switching temperature. These equations are now conventional difference equations, albeit involving the floor function, as opposed to the hybrid system we began with. Figures 2 and 2 show the results of some numerical simulations of (10). These figures show the time sequence obtained by iterating the return map (10) on  $[h_1 - r_2\tau, h_1]$ . The horizontal axis is (discrete) time, and the vertical axis is  $h$ , with parameters

as indicated in the captions. In Figure 2 the iterates appear to lie in a continuous interval of values which lies below  $h_1 = 18$ . The two time series shown in Figure 2 have a more complicated structure with clear evidence of bands: there are intervals of  $h$  which contain no iterates of the orbit shown. Note that the top of the uppermost band appear to be the threshold  $h_1$ .

The results certainly suggest that the motion is quasi-periodic, but there are also some less expected features: the banding is interesting. The closer the lower switching values are to  $h_1$  the better the control is working, and vice versa, so the banding suggests oscillation between efficient and inefficient operation of the thermostat. The bands will be explained in the next section, where we show that the analysis divides into two cases, one with bands and the other without. Further details of the special cases that arise in the banded case are pursued in subsequent sections.

### 3. Analysis of the map

The map (10) is in two parts:  $L : [h_1 - r_2\tau, h_1] \rightarrow (h_2, h_2 + r_1\tau]$  and  $R : (h_2, h_2 + r_1\tau] \rightarrow [h_1 - r_2\tau, h_1]$ . Due to the symmetry obtained by reversing the direction of temperature and exchanging subscripts we may assume that  $r_2 \geq r_1$  and hence that  $r_2\tau \geq r_1\tau$ . It has already been noted that these maps can be written using the floor function and are of the form  $h \rightarrow h + \alpha(h)$  where  $\alpha$  is piecewise constant, but it will be useful to spell this out explicitly. Define  $N_1$  by

$$h_1 + (N_1 - 1)r_1\tau \leq h_2 < h_1 + N_1r_1\tau \quad (11)$$

then the first map,  $L$ , is continuous on domains defined in terms of the points  $u_r$  where

$$u_r = h_2 - (N_1 + r)r_1\tau, \quad r = 0, \dots, k \quad (12)$$

with  $k$  defined by

$$h_2 - (N_1 + k + 1)r_1\tau < h_1 \leq h_2 - (N_1 + k)r_1\tau \quad (13)$$

The temperatures  $u_r$  are thus those which reach temperature  $h_2$  after time  $(N_1 + k - 1)r_1\tau$ . The map  $L$  is thus

$$L(x) = \begin{cases} x + (N_1 + k + 1)r_1\tau & \text{if } x \in [h_1 - r_2\tau, u_k], \\ x + (N_1 + r)r_1\tau & \text{if } x \in (u_r, u_{r-1}], \quad r = 1, \dots, k, \\ x + N_1r_1\tau & \text{if } x \in (u_0, h_1). \end{cases} \quad (14)$$

Note that the central branches of this map (if they exist) map the intervals  $(u_r, u_{r-1}]$  onto  $(h_2, h_2 + r_1\tau]$ .

Since  $r_1\tau \leq r_2\tau$  the image of the map  $R$  can have either one or two components ( $r_1\tau$  is the length of the domain of  $R$  and  $r_2\tau$  is the length of the range of  $R$ ). Let  $N_2$  be defined by

$$h_2 - N_2r_2\tau < h_1 \leq h_2 - (N_2 - 1)r_2\tau \quad (15)$$

The first case occurs if

$$h_2 + r_1\tau - N_2r_2\tau < h_1 \quad (16)$$

since in this case  $R$  is defined as

$$R(x) = x - N_2 r_2 \tau \quad (17)$$

If  $h_1 \leq h_2 + r_1 \tau - N_2 r_2 \tau$  then the image of  $R$  has two components:

$$R(x) = \begin{cases} x - N_2 r_2 \tau & \text{if } x \in (h_2, h_1 + N_2 r_2 \tau), \\ x - (N_2 + 1) r_2 \tau & \text{if } x \in [h_1 + N_2 r_2 \tau, h_2 + r_1 \tau]. \end{cases} \quad (18)$$

The choice made earlier to work with  $h < h_1$  as the criterion for switching on the heater rather than  $h \leq h_1$  leads to a slight anomaly in that if  $h_2 + r_1 \tau - N_2 r_2 \tau = h_1$ , i.e. equality holds in (16), then the second component of  $R$  in (18) is defined on a point. This complicates some features of the analysis and simplifies others. However, we can see that if (16) holds then the image of  $(h_2, h_2 + r_1 \tau]$  under  $R$  has one component, whilst if  $h_2 + r_1 \tau - N_2 r_2 \tau > h_1$  then it has two non-trivial components: these two cases correspond to the one band and two band solutions observed in the numerical experiments described earlier, as will be explained later. To determine the dynamics of the full system, the composition  $R \circ L$  needs to be analyzed.

### 3.1. Case I: $h_2 + r_1 \tau - N_2 r_2 \tau < h_1$

In this case the image of the upper interval is the single interval

$$J = (h_2 - N_2 r_2 \tau, h_2 + r_1 \tau - N_2 r_1 \tau] \quad (19)$$

in the lower interval, and hence when looking for recurrent dynamics we need only consider this subinterval. This interval has length  $r_1 \tau$  and since the distance between the points  $u_r$  is also  $r_1 \tau$ , and the distance between  $u_0$  and  $h_1$ , and  $h_1 - r_2 \tau$  and  $u_k$  are both less than  $r_1 \tau$ , the interval  $J$  contains one and only one of the points  $u_r$ ,  $u_m$  say, where

$$h_2 - N_2 r_2 \tau < u_m = h_2 - (N_1 + m) r_1 \tau \leq h_2 + r_1 \tau - N_2 r_1 \tau \quad (20)$$

Combining (14) and (17) gives  $R \circ L = T$  where

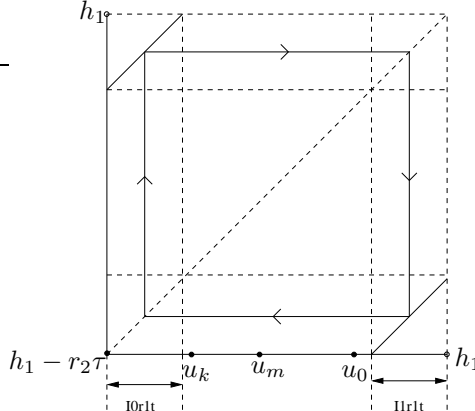
$$T(x) = \begin{cases} x + (N_1 + m + 1) r_1 \tau - N_2 r_2 \tau & \text{if } x \in (h_2 - N_2 r_2 \tau, u_m] \\ x + (N_1 + m) r_1 \tau - N_2 r_2 \tau & \text{if } x \in (u_m, h_2 + r_1 \tau - N_2 r_1 \tau] \end{cases} \quad (21)$$

Since  $u_m = h_2 - (N_1 + m) r_1 \tau$ ,  $R(u_m) = h_2 + r_1 \tau - N_2 r_2 \tau$ , and  $\lim_{x \downarrow u_m} T(x) = h_2 - N_2 r_2 \tau$ ,  $T$  is a rescaled circle map with rotation number  $\rho$  where<sup>1</sup>

$$1 - \rho = \frac{u_m - (h_2 - N_2 r_2 \tau)}{r_1 \tau}$$

---

<sup>1</sup>Here and below rotation numbers  $\rho$  are easily read off from the corresponding induced map defined on an interval  $[a, b]$  with ‘discontinuity’  $c \in (a, b)$  by noting that the rotation number is simply  $\rho = (b - c)/(b - a)$  or  $1 - \rho = (c - a)/(b - a)$ . This follows either from direct calculation or from the observation that the Haar (Lebesgue) measure is invariant under the map and the integer value of the lift of the map increase by one if an iterate falls in the interval  $(c, b]$ .

Figure 3. Representation of the map  $T(x)$  for Case I

or

$$\rho = \frac{(N_1 + m + 1)r_1\tau - N_2r_2\tau}{r_1\tau} \quad (22)$$

A map that arises in the current case is schematically represented in Fig. 3.1.

### 3.2. Case II: $h_2 + r_1\tau - N_2r_2\tau > h_1$

In this case the image of the upper interval intersects  $h_1$  after  $N_2$  iterations, but is not contained in  $[h_1 - r_2\tau, h_1]$  and so the image of the map  $R$  consists of two intervals:  $I_1 = [h_2 - N_2r_2\tau, h_1]$  on which the map is  $R(x) = x - N_2r_2\tau$ , and  $I_0 = [h_1 - r_2\tau, h_2 + r_1\tau - (N_2 + 1)r_2\tau]$  with  $R(x) = x - (N_2 + 1)r_2\tau$ . To consider recurrent behaviour we need to look at the map  $R \circ L$  on the union of these two intervals. Note that the difference between the lower endpoint of  $I_1$  and the upper endpoint of  $I_0$  is

$$(h_2 - N_2r_2\tau) - (h_2 + r_1\tau - (N_2 + 1)r_2\tau) = r_2\tau - r_1\tau > 0$$

so the two intervals do not intersect and there is a gap of length  $r_2\tau - r_1\tau$  between them. This is precisely the simple banding observed in the numerical experiments of the previous section. As in the previous section all recurrent behaviour can be described by restricting the dynamics to  $I_0 \cup I_1$ . Note that since the combined length of  $I_0$  and  $I_1$  is  $r_1\tau$  (the length of the upper interval), which is the distance between the  $(u_i)$ , and  $r_2\tau > r_1\tau$ , at most one of the points can lie in each interval  $I_j$ ,  $j = 0, 1$ . Hence  $u_i \in I_0 \cup I_1$  implies that  $i \in \{0, k\}$  and there are four cases to consider:

- all the points  $\{u_i\}$  lie in the gap;
- $u_0 \in I_1$  and  $u_k \notin I_0$ ;
- $u_0 \notin I_1$  and  $u_k \in I_0$ ; and
- $u_0 \in I_1$  and  $u_k \in I_0$ .

In the following two sections we will consider the first two cases. Such a presentation is sufficient to obtain an understanding of the complexity of the dynamics that can occur in our simple system. The remaining two cases can be considered in a like manner although with a proliferation of subcases and are omitted here for the sake of brevity.

The results proved above can be summarized by the following lemma.

**Lemma 3.1:** Consider the return map  $T = L \circ R$  defined by (14) and (17) or (18), defined on  $[h_1 - r_2\tau, h_1]$  derived from the thermostat model with  $r_2 > r_1$ . Define  $N_1$  and  $N_2$  as in (11) and (15). Then there are two cases:

- (a) If  $h_2 + r_1\tau - N_2 r_2 \tau < h_1$  (case 3.1) then the attractor is contained in a single interval and the return map restricted to this interval is, up to rescaling, a rigid rotation. If the rotation number is irrational then the dynamics is dense on this interval; if it is rational then every point is periodic.
- (b) If  $h_2 + r_1\tau - N_2 r_2 \tau \geq h_1$  (case 3.2) then the attractor is contained in two disjoint intervals, leading to the appearance of bands. Note that in the case of equality, one of these intervals is trivial: it is the single point  $h_1 - r_2\tau$ .

#### 4. All the points $\{u_i\}$ lie in the gap

This is the only one of the subcases enumerated above for which a short and simple argument provides a description of the dynamics. Even in this case there are four subcases which need to be treated separately.

Let us start with the case in which the points  $u_i$ ,  $i = 0, \dots, k$ , all lie in the gap between  $I_0$  and  $I_1$ . In this case  $u_k \geq h_2 + r_1\tau - (N_2 + 1)r_2\tau$

$$(N_1 + k + 1)r_1\tau \leq (N_2 + 1)r_2\tau \quad (23)$$

and  $u_0 \leq h_2 - N_2 r_2 \tau$  or, using (12)

$$N_2 r_2 \tau \leq N_1 r_1 \tau \quad (24)$$

which follows from the observation that  $u_0 = h_2 - N_1 r_1 \tau$  is less than the left hand end point of the  $N_2^{\text{th}}$  iterate of  $(h_2, h_2 + r_1\tau]$  which is just  $h_2 - N_2 r_2 \tau$ . Both the maps  $L|_{I_0}$  and  $L|_{I_1}$  are homeomorphisms:

$$L(x) = \begin{cases} x + (N_1 + k + 1)r_1\tau & \text{if } x \in I_0 \\ x + N_1 r_1 \tau & \text{if } x \in I_1 \end{cases} \quad (25)$$

and so

$$\begin{aligned} L(I_0) &= [h_1 - r_2\tau + (N_1 + k + 1)r_1\tau, h_2 + r_1\tau - (N_2 + 1)r_2\tau + (N_1 + k + 1)r_1\tau] \\ L(I_1) &= [h_2 - N_2 r_2 \tau + N_1 r_1 \tau, h_1 + N_1 r_1 \tau] \end{aligned} \quad (26)$$

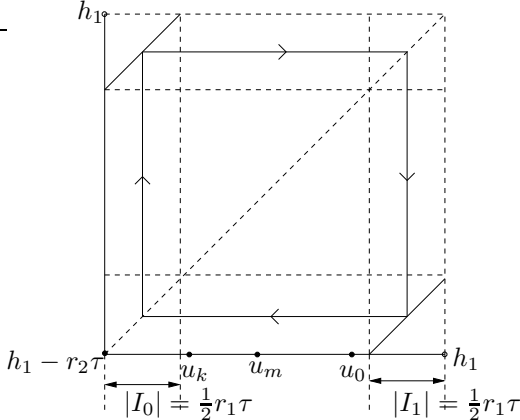
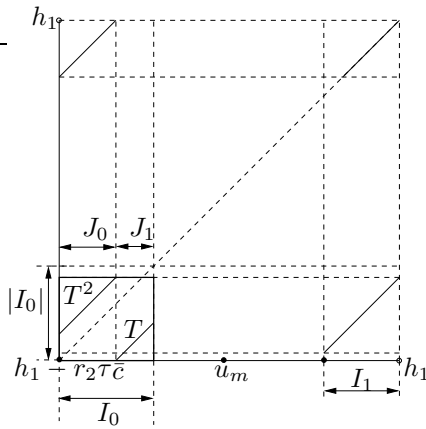
Now, by assumption  $R$  takes the form (18) and so we need to consider a number of cases depending on whether  $L(I_j)$  contains the discontinuity  $c = h_1 + N_2 r_2 \tau$ . Note that (23) implies that

$$h_1 - r_2\tau + (N_1 + k + 1)\tau < h_1 + N_2 r_2 \quad (27)$$

i.e. that the left hand end point of  $L(I_0)$  is to the left of  $c$ , and hence either  $c \in L(I_0)$  or  $L(I_0)$  lies to the left of  $c$ , in which case  $R|_{L(I_0)}$  is an isometry and  $R \circ L(I_0) \subseteq I_1$ . Similarly (24) implies that

$$h_1 + N_2 r_2 \leq h_1 + N_1 r_1 \tau \quad (28)$$

and so either  $c \in L(I_1)$  or  $L(I_1)$  lies to the right of  $c$ , in which case  $R|_{L(I_1)}$  is an isometry and  $R \circ L(I_1) \subseteq I_0$ .

Figure 4. Representation of the map  $T(x)$  for Case II subcase 4.1.Figure 5. Representation of the map  $T(x)$  in Case II subcase 4.2.  $T(x)$  acting on  $I_1$  is shown in the bottom right hand corner. The induced map  $T$  is shown in the bottom left hand corner.

#### 4.1. The case $c \notin L(I_0) \cup L(I_1)$

If  $c \notin L(I_0) \cup L(I_1)$  then  $|I_0| = |L(I_0)| = |R \circ L(I_0)|$ ,  $|I_1| = |L(I_1)| = |R \circ L(I_1)|$ ,  $|I_0| + |I_1| = r_1\tau$  and the properties of the isometry described above imply that  $c$  is the mid-point of  $[h_2, h_2 + r_1\tau]$  and  $T(I_0) = I_1$ ;  $T(I_1) = I_0$ . In this special case, then, all points in  $I_0 \cup I_1$  have period two under  $T$ . This is schematically depicted in Fig. 4.

#### 4.2. The case $c \in L(I_0)$ , $c \notin L(I_1)$

Since  $c \notin L(I_1)$ ,  $L(I_1)$  lies to the right of  $c$  and using the appropriate parts of (14) and (18) if  $x \in I_1$  then

$$T(x) = x + N_1 r_1 \tau - (N_2 + 1) r_2 \tau \quad (29)$$

so

$$T(I_1) = [h_2 - N_2 r_2 \tau + N_1 r_1 \tau - (N_2 + 1) r_2 \tau, h_1 + N_1 r_1 \tau - (N_2 + 1) r_2 \tau] \quad (30)$$

and is contained in  $I_0$ . Now,  $c \in L(I_0)$ , i.e.

$$h_1 - r_2 \tau + (N_1 + k + 1) r_1 \tau < h_1 + N_2 r_2 \tau < h_2 + r_1 \tau - (N_2 + 1) r_2 \tau + (N_1 + k + 1) r_1 \tau \quad (31)$$

so  $T(I_0)$  is in two parts, depending on whether  $x$  is to the right or left of the preimage of  $c$  under  $L|_{I_0}$ :  $\bar{c} = (h_1 + N_2 r_2) - (N_1 + k + 1)r_1 \tau$ : for  $x \in I_0$

$$T(x) = \begin{cases} x + (N_1 + k + 1)r_1 \tau - N_2 r_2 \tau & \text{if } x < \bar{c} \\ x + (N_1 + k + 1)r_1 \tau - (N_2 + 1)r_2 \tau & \text{if } x > \bar{c} \end{cases} \quad (32)$$

with  $T(x) \in I_0$  if  $x < \bar{c}$  and  $T(x) \in I_1$  if  $x > \bar{c}$ . Note that

$$\lim_{x \uparrow \bar{c}} T(x) = h_1 \quad \lim_{x \downarrow \bar{c}} T(x) = h_1 - r_2 \tau \quad (33)$$

The map  $T$  is sketched in Figure 5. To analyze this map we use the idea of renormalization (or induced maps) which has been used so effectively in the treatment of circle maps and beyond (e.g. [21, 22]). Define intervals  $J_0$  and  $J_1$  in  $I_0$  by

$$J_0 = [h_1 - r_2 \tau, \bar{c}) \quad J_1 = (\bar{c}, b] \quad (34)$$

where

$$b = T(h_1) = h_1 + N_1 r_1 \tau - (N_2 + 1)r_2 \tau \quad (35)$$

which is in  $I_0$  and define the induced map  $\mathcal{T}$  on  $J_0 \cup J_1$  by

$$\mathcal{T}(x) = \begin{cases} T^2(x) & \text{if } x \in J_0, \\ T(x) & \text{if } x \in J_1. \end{cases} \quad (36)$$

By equations (35) and (33),  $\mathcal{T}(\bar{c}_-) = b$  and  $\mathcal{T}(\bar{c}_+) = h_1 - r_2 \tau$  and  $\mathcal{T}$  has slope one everywhere, so it is a circle map with rotation number  $\rho_{\mathcal{T}} = (b - \bar{c})/(b - (h_1 - r_2 \tau))$ , i.e. on rearranging a little

$$\rho_{\mathcal{T}} = \frac{N_1 r_1 \tau - N_2 r_2 \tau}{(N_2 + 1)r_2 \tau - (N_1 + k + 1)r_1 \tau} - 1 \quad (37)$$

which can be viewed as the proportion of time an orbit spends in  $J_1$  under  $\mathcal{T}$ . To obtain the ‘rotation number’ of  $T$ ,  $\rho(T)$ , by which we mean the proportion of times an orbit spends in  $I_1$ , note that if  $x \in J_0$  (which is in  $I_0$ ) then  $T(x) \in I_1$  and  $T^2(x) = \mathcal{T}(x) \in I_0$ , and if  $x \in J_1$  then  $T(x) = \mathcal{T}(x) \in I_0$ . Hence an orbit of  $\mathcal{T}$  of length  $M$  which visits  $J_0 P_0$  times and  $J_1 P_1$  times (so  $P_0 + P_1 = M$ ) corresponds to an orbit of length  $2P_0 + P_1$  which visits  $I_0 P_0 + P_1$  times and  $I_1 P_0$  times, and so the proportion of visits to  $I_1$  is  $P_0/(2P_0 + P_1)$ . Now, as  $M \rightarrow \infty$ ,  $P_1/M \rightarrow \rho(\mathcal{T})$  and  $P_0/M \rightarrow 1 - \rho(\mathcal{T})$  and so

$$\rho(T) = \frac{1 - \rho(\mathcal{T})}{2 - \rho(\mathcal{T})} \quad (38)$$

which could be expressed in terms of the standard parameters using (37).

#### 4.3. The case $c \notin L(I_0)$ , $c \in L(I_1)$

This is essentially similar to the previous case, with the roles of  $I_0$  and  $I_1$  reversed.  $T$  is in two parts when restricted to  $I_1$ , and  $T|_{I_1}$  is the simple linear map

$$T(x) = x + (N_1 + k + 1)r_1 - N_2 r_2 \quad (39)$$

since  $L(I_0)$  lies to the left of  $c$ . Since  $c \in L(I_1)$  there exists  $c_1 \in I_1$  such that  $c_1 + N_1 r_1 = c$ , and for  $x \in I_1$

$$T(x) = \begin{cases} x + N_1 r_1 \tau - N_2 r_2 \tau & \text{if } x < c_1 \\ x + N_1 r_1 \tau - (N_2 + 1) r_2 \tau & \text{if } x > c_1 \end{cases} \quad (40)$$

So the induced map, defined on  $I_1$  this time is

$$\mathcal{T}(x) = \begin{cases} T(x) & \text{if } x < c_1 \\ T^2(x) & \text{if } x > c_1 \end{cases} \quad (41)$$

and restricted to an appropriate subinterval this is a circle map. The calculation of the rotation number is similar to the previous section and is omitted.

#### 4.4. The case $c \in L(I_0)$ , $c \in L(I_1)$

In this case  $T$  is in two parts when restricted to both  $I_0$  and  $I_1$ , and  $T|_{I_0}$  is given by (32) as before whilst  $T|_{I_1}$  is given by (40). Although this looks more complicated, it turns out that the calculations are the same as in previous cases. There are two cases, depending on the relative sizes of the intervals to the left of  $\bar{c}$  in  $I_0$  and to the right of  $c_1$  in  $I_1$ , i.e. on  $\bar{c} - h_1 + N_2 r_2$  and  $h_1 - c_1$ . If the first is smaller, then  $T([h_1 - N_2 r_2, \bar{c}])$  is contained in  $(c_1, h_1]$  and so no points can reach the interval in  $I_1$  to the left of  $c_1$  under iteration by  $T$  and the case is effectively equivalent to subsection 4.2, whilst if the order is opposite then the case is effectively equivalent to subsection 4.3. There is thus no need to consider this further.

### 5. Other cases

The remaining cases split into so many subcases that we believe that the interest derived from the results are not balanced by the time and effort required to describe them. We will briefly describe the dynamics for

$$u_0 \in I_1 \text{ and } u_k \notin I_0 \quad (42)$$

In this, the second of the four cases enumerated above,  $L|_{I_0}$  is a homeomorphism as in the previous section, whilst  $L|_{I_1}$  is in two parts:

$$L(I_1) = \begin{cases} x + N_1 r_1 \tau & \text{if } u_0 < x < h_1 \\ x + (N_1 + 1) r_1 \tau & \text{if } h_2 - N_2 r_2 \tau < x < u_0 \end{cases} \quad (43)$$

and note in passing that since  $u_0 = h_2 - N_1 r_1 \tau$  the assumption of this section is that

$$N_2 r_2 > N_1 r_1 \quad (44)$$

together with (23). Note further that since  $I_0 = [h_1 - r_2 \tau, h_2 + r_1 \tau - (N_2 + 1) r_2 \tau]$  we must have  $h_2 + r_1 \tau - (N_2 + 1) r_2 \tau - (h_1 - r_2 \tau) > 0$  or

$$h_2 - h_1 - N_2 r_2 \tau + r_1 \tau > 0 \quad (45)$$

This inequality has an important consequence.

**Lemma 5.1:** If  $u_0 \in I_1$  and  $u_k \notin I_0$  then  $L(I_1)$  consists of two disjoint intervals, and the point of discontinuity of  $R$ ,  $c = h_1 + N_2 r_2 \tau$ , lies above the lower of these.

*Proof:* Using (43),  $L(u_0, h_1) = (h_2, h_1 + N_1 r_1 \tau)$  and  $L(h_2 - N_2 r_2 \tau, u_0) = (h_2 - N_2 r_2 \tau + (N_1 + 1)r_1 \tau, h_2 + r_1 \tau)$ . These two intervals are disjoint provided

$$h_2 - N_2 r_2 \tau + (N_1 + 1)r_1 \tau > h_1 + N_1 r_1 \tau \quad (46)$$

i.e. provided

$$h_2 - h_1 - N_2 r_2 \tau + r_1 \tau > 0 \quad (47)$$

which is guaranteed by (45). The second part follows immediately from (44), which completes the proof of the lemma.

Of course, this means that if  $c$  is in one of the intervals making up  $L(I_1)$ , it must be in the upper one, and this will be the case provided

$$h_2 - N_2 r_2 \tau + (N_1 + 1)r_1 \tau < h_1 + N_2 r_2 \tau \quad (48)$$

or

$$h_2 - h_1 - N_2 r_2 \tau + r_1 \tau < N_2 r_2 \tau - N_1 r_1 \tau \quad (49)$$

Recall also that for  $x \in I_0$ ,

$$L(x) = x + (N_1 + k + 1)r_1 \tau \quad (50)$$

and by the argument already given to derive (27), either  $c \in L(I_0)$  or  $L(I_0)$  lies to the left of  $c$ . There we have therefore four subcases once again, but we will treat only one of these in any detail.

### 5.1. The case $c \notin L(I_0)$ and $c \notin L(I_1)$

It is a straightforward consequence of (23) that the left hand endpoint of  $L(I_0)$  is less than or equal to  $c$ , and hence that if  $c \notin L(I_0)$  then  $L(I_0)$  lies to the left of  $c$  and hence its image under  $R$  is in  $I_1$ . Moreover,  $T = R \circ L$  for  $x \in I_0$  is simply

$$T(x) = x + (N_1 + k + 1)r_1 \tau - N_2 r_2 \tau \quad (51)$$

In the right hand interval of  $I_1$ ,  $I_1^R$  say,  $L(I_1^R)$  is to the left of  $c$  and so its image under  $R$  is also in  $I_1$  and for  $x \in I_1^R$

$$T(x) = x + N_1 r_1 \tau - N_2 r_2 \tau \quad (52)$$

and  $T(I_1^R) = (h_2 - N_2 r_2 \tau, h_1 + N_1 r_1 \tau - N_2 r_2 \tau)$ . Finally the image of the left hand interval of  $I_1$ ,  $I_1^L$  say, under  $L$  is above  $c$ , so the image under  $T = R \circ L$  lies in  $I_0$  with

$$T(x) = x + (N_1 + 1)r_1 \tau - (N_2 + 1)r_2 \tau \quad (53)$$

for  $x \in I_1^L$ , and  $T(I_1^L) = (h_2 + (N_1 + 1)r_1 \tau - r_2 \tau, h_2 + r_1 \tau - (N_2 + 1)r_2 \tau)$  and so the right hand end point of this interval is the right hand end point of  $I_0$ . Since

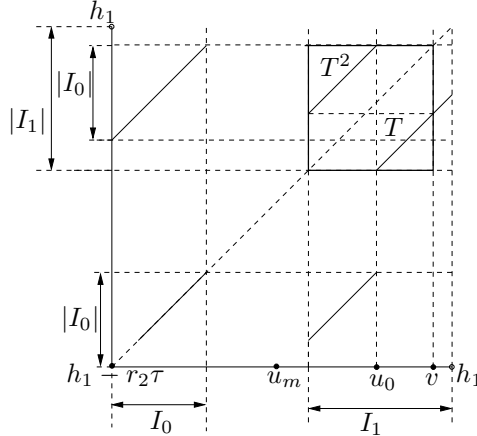


Figure 6. Representation of the map  $T(x)$  in Case II subcase 5.1.  $T(x)$  acting on  $I_0$  is shown in the bottom left hand corner. The induced map  $\mathcal{T}$  is shown in the upper right hand corner.

$v = T^2(h_2 + r_1\tau - (N_2 + 1)r_2\tau) > u_0$  we can define the induced map  $\mathcal{T}$  as

$$\mathcal{T} = \begin{cases} T^2(x) & \text{if } h_2 - N_2r_2\tau < x < u_0 \\ T(x) & \text{if } u_0 < x < v \end{cases} \quad (54)$$

Then  $\mathcal{T}$  captures the recurrent dynamics of  $T$  and is a circle map with rotation number

$$\rho(\mathcal{T}) = \frac{v - u_0}{v - h_2 - N_2r_2\tau} \quad (55)$$

from which the standard argument shows that the proportion of time spent in  $I_1$  by an orbit under  $T$  is  $\rho(T)$  given by

$$\rho(T) = \frac{\rho(\mathcal{T})}{2 - \rho(\mathcal{T})} \quad (56)$$

The action of the map  $T(x)$  on the points in the intervals  $I_0$  and  $I_1$  is schematically depicted in Fig. 6. The remaining subcases for the case (42) require a great deal more effort, and so the details, and the description of the dynamics for the remaining cases, has not been attempted in detail. We pass on to the general case where the dynamics is defined by nonlinear differential equations.

## 6. The General Case

The dynamics of the linear model described above gives a sense of the different behaviours which can be expected with digital sampling, but some features are due to the linear nature of the flow, and so it is worth making some limited remarks about the more general case

$$\frac{dh}{dt} = \begin{cases} f(h) & \text{if } c = \text{on} \\ -g(h) & \text{if } c = \text{off} \end{cases} \quad (57)$$

where  $f$  and  $g$  are strictly positive functions on their domains of definition. Changing our notation for the thresholds, so  $c$  changes from **on** to **off** if  $h$  rises above  $\alpha$  (which was  $h_2$ ) and from **off** to **on** if  $h$  falls below  $b$  (which was  $h_1$ ),  $b < \alpha$ , then if the control is on and temperature sampled at regular time intervals  $\tau$  for some

fixed  $\tau > 0$ , the highest the temperature can rise to is  $\beta$  where

$$\int_{\alpha}^{\beta} \frac{dh}{f(h)} = \tau \quad (58)$$

Similarly, the lowest the temperature can fall is  $a$  defined by

$$\int_a^b \frac{dh}{g(h)} = \tau \quad (59)$$

Now let  $\phi_f(h_0, t)$  be the solution of the **on** equation at time  $t$  with initial condition  $h = h_0$ , and  $\phi_g(h_0, t)$  the equivalent solution flow for the **off** equation. Thinking about the initial increase in temperature from  $a$  define  $\tau_f$  by

$$\int_a^b \frac{dh}{f(h)} = \tau_f \quad (60)$$

and, similarly,  $\tau_g$  by

$$\int_{\alpha}^{\beta} \frac{dh}{g(h)} = \tau_g \quad (61)$$

so that

$$\phi_f(a, \tau_f) = b \quad \phi_g(\beta, \tau_g) = \alpha \quad (62)$$

and so, using the standard group property of the flows,

$$\phi_f(a, t + \tau_f) = \phi_f(b, t) \quad \phi_g(\beta, t + \tau_g) = \phi_g(\alpha, t) \quad (63)$$

Equations (58) and (59) are equivalent to

$$\phi_f(\alpha, \tau) = \beta, \quad \phi_g(b, \tau) = a \quad (64)$$

The arguments are going to be analogous to those of the previous sections, although (not surprisingly) rather more possibilities can arise. Define  $N_f$  and  $N_g$  to be the least positive integers such that

$$\phi_f(b, N_f \tau) > \alpha, \quad \phi_g(\alpha, N_g \tau) < b \quad (65)$$

and (cf. the definition of the points  $u_i$ ) let

$$M_f = \text{card } ([\cup_{n \geq 0} \phi_f(\alpha, -n\tau)] \cap [a, b)) \quad (66)$$

and

$$M_g = \text{card } ([\cup_{n \geq 0} \phi_g(b, -n\tau)] \cap [\alpha, \beta)) \quad (67)$$

We now want to derive return maps on the interval  $[a, b)$  as in previous sections. Some cases are easy to describe.

**Lemma 6.1:** *If  $M_f = M_g = 0$  then the return map has at least one attracting fixed point.*

*Proof:* Since  $M_f = 0$ ,  $\phi_f(a, N_f\tau) > \alpha$  or there would be a preimage of  $\alpha$  in  $[a, b]$ . Hence  $\phi_f([a, b], N_f\tau) \subset [\alpha, \beta]$ . Similarly,  $M_g = 0$  implies that  $\phi_g([\alpha, \beta], N_g\tau) \subset [a, b]$ . The return map  $T$  thus has  $T([a, b]) \subset [a, b]$  and is monotonic and increasing as  $x < y$  implies  $\phi_f(x, t) < \phi_f(y, t)$ . Thus  $T$  has at least one stable fixed point, and all iterates of the map are asymptotically fixed.

At the opposite extreme there can be chaos.

**Lemma 6.2:** *If  $M_f \geq 2$  and  $M_g \geq 3$  (or  $M_f \geq 3$  and  $M_g \geq 2$ ) then the return map is chaotic.*

*Proof:* If  $M_f \geq 2$  then let  $u_0$  be such that  $u_0 = \phi_f(\alpha, -N_f\tau)$  and  $u_1 = \phi_f(u_0, -\tau)$ . Note that  $a \leq u_1 < u_0 < b$ . Moreover,  $\phi_f((u_1, u_0), (N_f + 1)\tau) = (\alpha, \beta)$ . Similarly, since  $M_g \geq 3$  there exist  $v_0 < v_1 < v_2$  in  $[\alpha, \beta]$  such that

$$\phi_g((v_0, v_1), (N_f + 1)\tau) = \phi_g((v_1, v_2), (N_f + 2)\tau) = (a, b) \quad (68)$$

The return map  $T$  on  $[a, b]$  is therefore such that the image of  $(u_1, u_0)$  covers itself twice and the dynamics contains an invariant set equivalent to a full shift on two symbols – possibly with a countable number of orbits removed because the intervals are open. This is the one-dimensional equivalent of the horseshoe, a hallmark of chaos.

The intermediary cases are more complicated. For example, if  $M_f = 0$  and  $M_g = 1$  then  $\phi_f((a, b), N_f\tau) \subset (\alpha, \beta)$ , and the single preimage of  $b$  in  $[\alpha, \beta]$  is either in  $\phi_f((a, b), N_f\tau)$  or it is not. In the latter case  $T$  is a monotonic map and the attractor a fixed point as in Lemma 6.1. In the former case  $T$  is a piecewise monotonic map with a single discontinuity. This class contains the slope one maps described above, but include a range of more complicated dynamics and transitions to chaos as described in [23, 24].

Note that some of the more abstract conditions here can be expressed in terms of the parameters. For example the following lemma connects the condition  $M_f = 0$  with an inequality between  $\tau$  and  $\tau_f$ .

**Lemma 6.3:** *If  $M_f = 0$  then  $\tau > \tau_f$ .*

*Proof:* If  $M_f = 0$  then

$$\alpha < \phi_f(a, N_f\tau) < \phi_f(b, N_f\tau) \leq \beta = \phi(\alpha, \tau) \quad (69)$$

Flowing back through time  $-N_f\tau$  under  $f$  this implies that

$$\phi_f(\alpha, -N_f\tau) < \phi_f(a, 0) < \phi_f(b, 0) \leq \phi(\alpha, (-N_f + 1)\tau) \quad (70)$$

Taking the last inequality and flowing back an additional  $-\tau$  and then using the first inequality and the definition of  $\tau_f$  gives

$$\phi_f(b, -\tau) \leq \phi(\alpha, -N_f\tau) < \phi_f(a, 0) = \phi_f(b, -\tau_f) \quad (71)$$

and taking the inequality  $\phi_f(b, -\tau) < \phi_f(b, -\tau_f)$  and flowing through  $\tau$  for clarity,  $\phi_f(b, 0) < \phi_f(b, \tau - \tau_f)$ . Since  $f$  is strictly positive this implies that  $\tau - \tau_f > 0$  as required.

No doubt other more complicated connections can be made, but these results establish the principles under which the general cases could be elucidated.

## 7. Conclusions

In the paper we studied the dynamics of a simple one-dimensional on/off control system where the control variable was given at discrete time intervals. In the case when the system evolution was assumed linear in the on and off states we were able to obtain a re-scaled circle map that captures the system dynamics. We have shown that depending on the system parameters we might encounter a family of periodic orbits, quasi-periodic oscillations or a banding structure of quasi-periodicity. Using equivalent methodology to that which allowed us to study the linear case we extended the analysis to the case when the system evolution is governed by generic non-linear functions. In particular, we have shown that a fixed point attractor and chaotic dynamics are present in this more general case. Some results that link the sampling time with the width of the interval on which the asymptotic dynamics might settle have been also presented (see Lemma 4).

Further investigations are directed toward understanding of delay, hysteretic and stochastic effects on the dynamics of systems with continuous and discrete transitions where digital sampling of a state/control variable is used.

## References

- [1] B. Brogliato. *Nonsmooth Mechanics – Models, Dynamics and Control*. Springer–Verlag, New York, 1999.
- [2] B. Blazejczyk-Okolewska, K. Czolczynski, and J. Kapitaniak, T. Wojewoda. *Chaotic Mechanics is Systems with Impacts and Friction*. World Scientific, Singapore, 1999.
- [3] B. Brogliato. *Impacts in Mechanical Systems – Analysis and Modelling*. Springer–Verlag, New York, 2000. Lecture Notes in Physics, Volume 551.
- [4] M. di Bernardo, C. J. Budd, A. R. Champneys, and P. Kowalczyk. *Piecewise-smooth Dynamical Systems. Theory and Applications*, volume 163. Springer–Verlag, New York, 2007.
- [5] W.P.M.H. Heemels and B.B. Brogliato. The complementarity class of hybrid dynamical systems. *European Journal of Control*, 9:311–319, 2003.
- [6] S. Banerjee and G. Verghese. *Nonlinear Phenomena in Power Electronics*. IEEE press, New York, 2001.
- [7] M. di Bernardo, K. H. Johansson, and F. Vasca. Self-oscillations and sliding in relay feedback systems: Symmetry and bifurcations. *International Journal of Bifurcations and Chaos*, 11(4):1121–1140, 2001.
- [8] A. B. Nordmark. Non-periodic motion caused by grazing incidence in impact oscillators. *Journal of Sound and Vibration*, 2:279–297, 1991.
- [9] C. Budd, K.A. Cliffe, and F. Dux. The effect of frequency and clearance variations on one-degree of freedom impact oscillators. *J. Sound & Vibration*, 184, 1995.
- [10] C.J. Budd and A.G. Lee. Double impact orbits of periodically forced impact oscillators. *Proc. Roy. Soc. Lond. A*, 452, 1996.
- [11] M. H. Frederiksson and A. B. Nordmark. Bifurcations caused by grazing incidence in many degrees of freedom impact oscillators. *Proc. Royal Soc. Lond. A*, 453:1261–1276, 1997.
- [12] K. Popp, N. Hinrichs, and M. Oestreich. Dynamical behaviour of friction oscillators with simultaneous self and external excitation. *Sadhana (Indian Academy of Sciences)*, 20:627–654, 1995.
- [13] L. N. Virgin and C. J. Begley. Grazing bifurcations and basins of attraction in an impact-friction oscillator. *Physica D*, 130:43–57, 1999.
- [14] M. di Bernardo, P. Kowalczyk, and A. Nordmark. Sliding bifurcations: A novel mechanism for the sudden onset of chaos in dry-friction oscillators. *International Journal of Bifurcation and Chaos*, 13(10):2935–2948, 2003.
- [15] Ogata Katsuhiko. *Modern Control Engineering*. Tom Robbins, Fourth Edition, 2002.
- [16] Tetsuro Tanaka, Tamotsu Ninomiya, and Koosuke Harada. Random-switching control in dc-to-dc converters. *Appears in Power Electronics Specialists Conference, 1989, PESC '89 Record*, 1:500–507, 1989.
- [17] J. Sieber, P. Kowalczyk, S.J. Hogan, and M. di Bernardo. Dynamics of symmetric dynamical systems with delayed switching. *Special Issue of Journal of Vibration and Control on Dynamics and Control of Systems with Time-Delay (accepted)*, 2008.
- [18] Kyung-Sup Lee and Abraham H. Haddad. Stabilization of discrete-time quantized control system. In *Proceedings of the American Control Conference*, pages 3506–3511, 2002.
- [19] J. H. Braslavsky, E. Kofman, and F. Felicioni. Effects of time quantization and noise in level crossing sampling stabilization. In *In Proceedings of AADECA*, 2006.
- [20] D. Liberzon. Quantization, time delays, and nonlinear stabilization. *IEEE TRANSACTIONS ON AUTOMATIC CONTROL*, 51(7):1190–1195, July 2006.
- [21] J.M. Gambaudo, O. Lanford III, and C. Tresser. Dynamique symbolique des rotations. *C. R. Acad. Sc. Paris*, 299 Série I:823–826, 1984.
- [22] P. Veerman. Symbolic dynamics and rotation numbers. *Journal of Physics A*, 134(3):543–576, 1986.

- [23] J.M.Gambaudo, I. Procaccia, S. Thomae, and C. Tresser. New universal scenarios for the onset of chaos in lorenz-type flows. *Phys. Rev. Lett.*, 57:925–928, 1987.
- [24] C. Tresser. Nouveaux types de transitions vers une entropie topologique positive. *C.R.Acad. Sci. (Paris) Série I*, 296:729–732, 1983.

## 8. Acknowledgements

Research partially funded by EPSRC grant EP/E050441/1 and the University of Manchester.